

LIGHT-MANAGEMENT STRATEGIES FOR THIN-FILM SILICON MULTIJUNCTION SOLAR CELLS

Bjoern Niesen,¹ Jan-Willem Schüttauf,¹ Etienne Moulin,¹ Simon Hänni,¹ Mathieu Boccard,¹ Elmar Feuser,¹ Xavier Niquille, Michael Stuckelberger,¹ Nicolas Blondiaux,² Raphaël Pugin,² Emmanuel Scolan,² Fanny Meillaud,¹ Franz-Josef Haug,¹ Aïcha Hessler-Wyser,^{1,3} and Christophe Ballif^{1,2}

1. Photovoltaics and Thin Film Electronics Laboratory, Institute of Microengineering (IMT), Ecole Polytechnique Fédérale de Lausanne (EPFL), Rue de la Maladière 71, CH-2002 Neuchâtel, Switzerland

2. Centre Suisse d'Electronique et de Microtechnique (CSEM) SA, Rue Jaquet-Droz 1, CH-2002 Neuchâtel, Switzerland

3. Centre Interdisciplinaire de Microscopie Electronique (CIME), Ecole Polytechnique Fédérale de Lausanne (EPFL), CH-1015 Lausanne, Switzerland

ABSTRACT

Light management is of crucial importance to reach high efficiencies with thin-film silicon multijunction solar cells. In this contribution, we present light-management strategies that we recently developed. This includes high quality absorber materials, low-refractive index intermediate reflectors, and highly transparent multiscale electrodes. Specifically, we show the fabrication of high-efficiency tandem devices with a certified stabilized efficiency of 12.6%, triple-junction solar cells with a stabilized efficiency of 12.8%, recently developed smoothing intermediate reflector layers based on silicon dioxide nanoparticles, and periodic-on-random multiscale textures.

1. INTRODUCTION

The optimization of multijunction thin-film silicon solar cells requires accurate tuning of the photocurrents generated by the individual sub cells. Light-management strategies involve (i) the choice of absorber materials, (ii) the number of junctions, (iii) the utilization of reflecting and anti-reflecting layers, (iv) the texturing of interfaces, (v) the minimization of parasitic losses, and (vi) the minimization of light-induced degradation. The aim of these strategies lies in enhancing the summed photocurrent without reducing the open-circuit voltage (V_{oc}), as well as finding the ideal balance between a maximized short-circuit current density (J_{sc}), obtained at matched sub-cell current densities, and a maximal stabilized fill factor (FF), reached when the sub cell with the highest material quality becomes strongly current limiting.

Here, we present several light-management strategies to optimize the power conversion efficiency (η) of multijunction thin-film silicon solar cells in p-i-n configuration. We show several absorber materials for high-efficiency triple-junction cells, and present recent progress on intermediate reflectors, including

nanoparticle-based reflectors that do not only redistribute photocurrent generation between the sub cells, but also reduce interface roughness, enhancing the material quality of the absorber layers. Finally, we show multiscale transparent front electrodes in hydrogenated amorphous silicon (a-Si:H)/ microcrystalline silicon ($\mu\text{c-Si:H}$) tandem devices.

2. ABSORBER MATERIALS

Over the past years, several high-quality thin-film silicon absorber layers have been developed [1-4]. These include a-Si:H layers deposited over a very wide range of process parameters. For application in multijunction devices, we have explored the full spectrum of deposition conditions for a-Si:H layers, leading to a V_{oc} of 1.04 V or to a J_{sc} of 19.5 mA/cm² [5]. The former cell is highly interesting for application as a top cell in triple- or quadruple-junction devices, whereas the latter could find application in a-Si:H/ $\mu\text{c-Si:H}$ tandem cells. For $\mu\text{c-Si:H}$ cells, we obtained a certified efficiency as high as 10.7% [6] as well as a $V_{oc} > 600$ mV with a thin absorber layer and passivated interfaces [Hänni thesis 2014]. Such cells could be used as middle cells in triple-junction devices. Furthermore, we recently developed high-quality a-SiGe:H-based cells [7].

With these building blocks, we made triple-junction solar cells with stabilized efficiencies of up to 11.3% for a-Si:H/a-SiGe:H/ $\mu\text{c-Si:H}$ devices (see Fig. 1) and 12.8% for a-Si:H/ $\mu\text{c-Si:H}$ / $\mu\text{c-Si:H}$ cells (Fig. 2) [7,8]. Recently, we also presented quadruple-junction cells. Even though current matching and reducing parasitic losses are challenging for such devices, we believe they offer the potential to reach stabilized efficiencies above 14% [7]. To improve the summed photocurrent in triple- or quadruple-junction cells further, bottom cells with a very high infrared response were developed, using SiF₄ as a source gas [9-11]. This approach led to tandem cells with a summed J_{sc} as high as 31.9 mA/cm² [11].

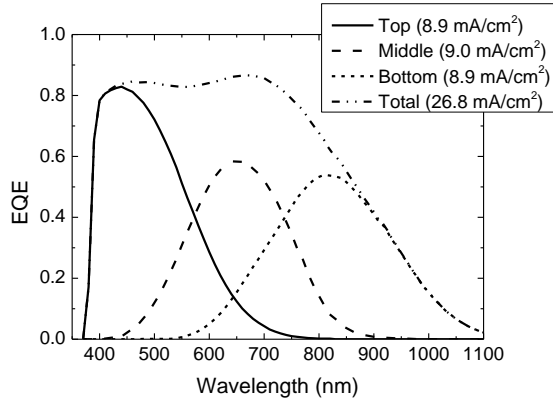


Fig. 1: a-Si:H/a-SiGe:H/ μ c-Si:H triple-junction solar cell. Layer stack: Top cell: a-Si:H, 130 nm thick; middle cell: a-SiGe:H, 220 nm thick; SiO_x intermediate reflector, 115 nm thick; bottom cell: μ c-Si:H, 2.6 μm thick. $V_{oc} = 2.00$ V, $J_{sc} = 8.9$ mAcm^{-2} , FF = 63.5%, $\eta = 11.3\%$ (all values after > 1000 h of light soaking).

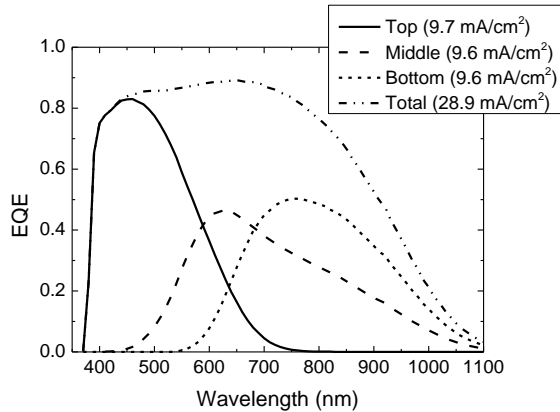


Fig. 2: a-Si:H/ μ c-Si:H/ μ c-Si:H triple-junction solar cell. Layer stack: top cell: a-Si:H, 140 nm thick; middle cell: μ c-Si:H, 1.5 μm thick; bottom cell: μ c-Si:H, 2.6 μm thick. $V_{oc} = 1.85$ V, $J_{sc} = 9.6$ mAcm^{-2} , FF = 72.5%, $\eta = 12.8\%$ (all values after > 1000 h of light soaking).

3. INTERMEDIATE REFLECTORS

In multijunction solar cells, intermediate reflectors are frequently used to redistribute the photocurrent generation between individual sub cells [12,13]. This is especially important to obtain high photocurrents in a-Si:H and a-SiGe:H sub cells even for thin absorber layers, which reduces light-induced degradation. Recently, we achieved a certified world-record stabilized efficiency of 12.63% for a-Si:H/ μ c-Si:H tandem cells with an improved low-refractive index SiO_x intermediate reflector (Fig. 3) [14]. By tuning the $\text{CO}_2:\text{SiH}_4$ ratio during the SiO_x layer deposition, a refractive index as low as 1.75 was reached.

Intermediate reflectors cannot only be employed to redistribute the photocurrent between the sub cells, but can also be made non-conformal, such that the surface morphologies between the two adjacent sub cells are

decoupled. In p-i-n multijunction cells this is particularly interesting at an interface between an a-Si:H or a-SiGe:H cell and a μ c-Si:H cell, where the intermediate reflector can planarize the interface and thus provide a smoother growth substrate for the μ c-Si:H cell, resulting in an improved electrical quality of the μ c-Si:H material.

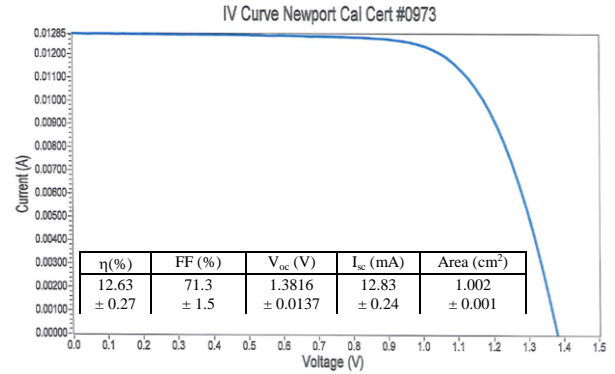


Fig. 3: Certified stabilized current-voltage characteristics and device parameters of an a-Si:H/ μ c-Si:H tandem cell with low-refractive index SiO_x intermediate reflector.

A novel intermediate reflector based on a self-patterned layer of SiO_2 nanoparticles deposited by solution processing was recently demonstrated [15]. By adjusting the SiO_2 nanoparticle dispersion formulation and spin-coating parameters, a valley-filling effect was obtained on rough substrates, such that small surface features were covered by a dense SiO_2 nanoparticle layer with a flat surface while large surface features penetrated the electrically insulating SiO_2 nanoparticle layer, allowing for efficient charge transport between the two sub cells (Fig. 4).

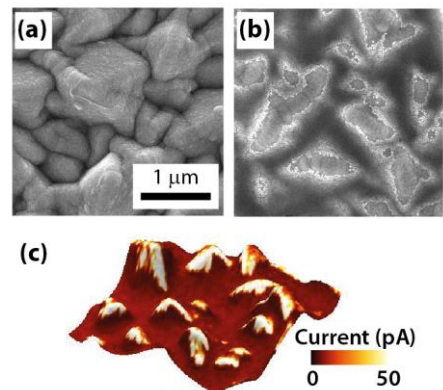


Fig. 4: a, b) Top-view scanning electron microscopy images of the a-Si:H cell surface (a) and the SiO_2 nanoparticle intermediate reflector layer deposited on the a-Si:H cell (b). c) Height/current flow image as obtained by conductive atomic force microscopy of the SiO_2 nanoparticle intermediate reflector on the a-Si:H cell surface. The color scale indicates the current flowing between the surface and the tip of the atomic force microscope.

By depositing such a self-patterned SiO_2 nanoparticle layer as an intermediate reflector in an a-Si:H/ $\mu\text{c-Si:H}$ tandem cell, the V_{oc} could be significantly improved as compared to a reference tandem cell without an intermediate reflector and the photocurrent was efficiently redistributed between the two sub cells (Fig. 5 and Table I). This photocurrent redistribution could be readily tuned by varying the thickness of the SiO_2 nanoparticle layer.

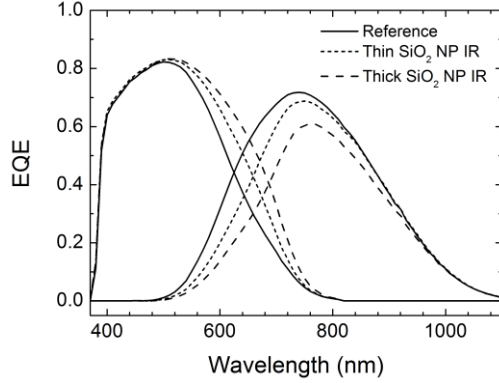


Fig. 5: External quantum efficiency (EQE) spectra of pristine a-Si:H (230-nm-thick intrinsic layer)/ $\mu\text{c-Si:H}$ (1.6- μm -thick intrinsic layer) tandem cells without intermediate reflector (reference), and with a thin or thick SiO_2 nanoparticle intermediate reflector (SiO_2 NP IR). All cells were deposited on 3.5- μm -thick ZnO front electrodes, deposited by low-pressure chemical vapor deposition.

Table I. Device parameters of pristine a-Si:H/ $\mu\text{c-Si:H}$ tandem cells shown in Fig. 5.

	$J_{sc}(\text{mAcm}^{-2})$	$V_{oc}(\text{mV})$	FF(%)	$\eta(\%)$
Reference	12.00	1358	70.1	11.42
Thin NP IR	12.33	1363	73.8	12.40
Thick NP IR	10.36	1381	79.8	11.42

4. MULTISCALE ELECTRODES

The optimization of thin-film silicon solar cells grown on textured electrodes involves a trade-off between maximizing photocurrent and minimizing detrimental effects to the electrical quality of the absorber layers. In multijunction devices, this trade-off is complicated by the fact that light incoupling and trapping has to be optimized for several sub cells. Multiscale textures have been developed to address this issue [16-18]. We recently combined random and 2-D periodic textures into a multiscale texture (Fig. 6) [19]. In particular, by adding a micrometer-scale texture to a submicron-scale textured ZnO front electrode grown by low-pressure chemical vapour deposition, we were able to reduce the front-electrode thickness to less than 1 μm

while maintaining cell performance at an excellent level (Fig. 7).

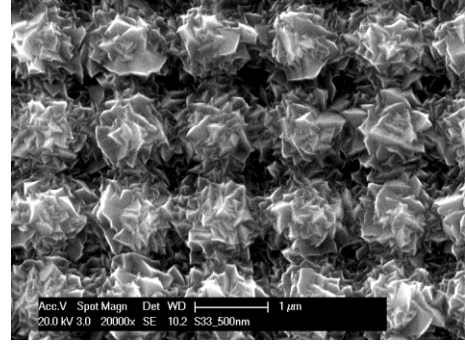


Fig. 6: Scanning electron micrograph of a double-texture front electrode combining a 2-D periodic texture and a randomly textured 0.5- μm -thick ZnO layer grown by low-pressure chemical vapor deposition.

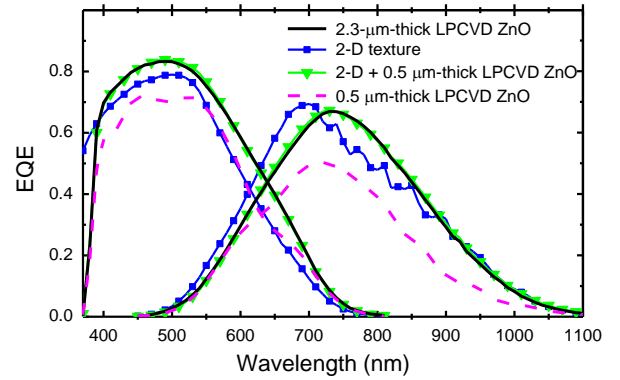


Fig. 7: EQE of a-Si:H/ $\mu\text{c-Si:H}$ tandem solar cells deposited on 2.3- μm -thick ZnO grown by low-pressure chemical vapor deposition (LPCVD), a 2-D periodic texture (with a period of 1.2 μm and an aspect ratio of 0.3), and the superposition of the 2-D texture and a 0.5- μm -thick LPCVD-ZnO layer. To illustrate the beneficial effect of the combined texture, the EQE of a cell on a 0.5- μm -thick LPCVD-ZnO layer is also shown.

5. CONCLUSIONS

We presented several strategies to optimize the light management in multijunction thin-film silicon solar cells. We developed several absorber materials for use in multijunction cells. Specifically, high-voltage a-Si:H cells as top cells, high voltage $\mu\text{c-Si:H}$ cells with very thin a-Si:H passivation layers as middle cells, and high-infrared-current $\mu\text{c-Si:H}$ cells deposited using SiF_4 instead of SiH_4 as a precursor gas as bottom cells. We presented the recent development of low-refractive index SiO_x intermediate reflectors that led to a record stabilized efficiency in tandem cells, as well as low-refractive index smoothening intermediate reflectors based on self-patterned SiO_2 nanoparticle layers that do

not only efficiently redistribute photocurrent but also improve the electrical quality of the $\mu\text{-Si:H}$ bottom cell. Finally, we demonstrated random-on-periodic multiscale textures that enable excellent optical performance while maintaining a high V_{oc} for front-electrode thicknesses of less than 1 μm .

ACKNOWLEDGEMENTS

Support by the Swiss Commission for Technology and Innovation (CTI) under project number 13333.1 (TRIGGER), the Swiss Federal Energy Office under project no SI/500750-01, and the Velux Stiftung is gratefully acknowledged. A part of this work was carried out in the framework of the FP7 project "Fast Track", funded by the EC under grant agreement no 283501.

REFERENCES

- [1] T. Matsui, H. Sai, K. Saito, and M. Kondo, *Prog. Photovolt: Res. Appl.* **21**, 1363 (2013).
- [2] M. Stuckelberger, M. Despeisse, G. Bugnon, J.-W. Schüttauf, F.-J. Haug, and C. Ballif, *J. Appl. Phys.* **114**, 154509 (2013).
- [3] G. Bugnon, G. Parascandolo, T. Soderstrom, P. Cuony, M. Despeisse, S. Hänni, J. Holovsky, F. Meillaud, and C. Ballif, *Adv. Funct. Mater.* **22**, 3665 (2012).
- [4] S. Guha, J. Yang, B. Yan, *Sol. Energy Mater. Sol. Cells* **119**, 1 (2013).
- [5] M. Stuckelberger, A. Billet, Y. Riesen, M. Boccard, M. Despeisse, J.-W. Schüttauf, F.-J. Haug, and C. Ballif, *Prog. Photovolt.: Res. Appl.* DOI:10.1002/pip.2559.
- [6] S. Hänni, G. Bugnon, G. Parascandolo, M. Boccard, J. Escarré, M. Despeisse, F. Meillaud, and C. Ballif, *Prog. Photovolt.: Res. Appl.* **21**, 821 (2013).
- [7] J.-W. Schüttauf, B. Niesen, L. Löfgren, M. Bonnet-Eymard, M. Stuckelberger, S. Hänni, M. Boccard, G. Bugnon, M. Despeisse, F.-J. Haug, F. Meillaud, and C. Ballif, *Sol. Energy Mater. Sol. Cells*, DOI: 10.1016/j.solmat.2014.11.006.
- [8] J.-W. Schüttauf, G. Bugnon, M. Stuckelberger, S. Hänni, M. Boccard, M. Despeisse, F.-J. Haug, F. Meillaud, and C. Ballif, *IEEE J. Photovolt.* **4**, 757 (2014).
- [9] J.-C. Dornstetter, S. Kasouit, and P. Roca i Cabarrocas, *IEEE J. Photovolt.* **3**, 581 (2013).
- [10] S. Hänni, J. Persoz, B. Niesen, M. Boccard, G. Bugnon, J.-W. Schüttauf, M. Ledinsky, L. Löfgren, J. Bailat, F.-J. Haug, F. Meillaud, and C. Ballif "Highly crystalline microcrystalline silicon solar cells for enhanced near-infrared absorption", *Technical Digest of the 6th World Conference on Photovoltaic Energy Conversion* (2014).
- [11] Simon Hänni, PhD thesis, EPFL, (2014).
- [12] K. Yamamoto, A. Nakajima, M. Yoshimi, T. Sawada, S. Fukuda, T. Suezaki, M. Ichikawa, Y. Koi, M. Goto, T. Meguro, T. Matsuda, T. Sasaki, and Y. Tawada, *Proceedings of the 4th World Conference on Photovoltaic Energy Conversion*, p.1489 (2006).
- [13] A. Lambertz, T. Grundler, and F. Finger, *J. Appl. Phys.* **109**, 113109 (2011).
- [14] M. Boccard, M. Despeisse, J. Escarre, X. Niquille, G. Bugnon, S. Hänni, M. Bonnet-Eymard, F. Meillaud, C. Ballif, *IEEE J. Photovolt.* **4**, 1368 (2014).
- [15] B. Niesen, N. Blondiaux, M. Boccard, M. Stuckelberger, R. Pugin, E. Scolan, F. Meillaud, F.-J. Haug, A. Hessler-Wyser, and C. Ballif, *Nano Lett.* **14**, 5085 (2014).
- [16] M. Kambe, K. Masumo, N. Taneda, T. Oyama & K. Sato. *Technical Digest of the 17th International Photovoltaic Science and Engineering Conference*, p. 1161 (2007).
- [17] M. Boccard, C. Battaglia, S. Hänni, K. Söderström, J. Escarré, S. Nicolay, F. Meillaud, M. Despeisse, and C. Ballif, *Nano Lett.* **12**, 1344 (2012).
- [18] H. Tan, E. Psomadaki, O. Isabella, M. Fischer, P. Babal, R. Vasudevan, M. Zeman, and A. H. M. Smets, *Appl. Phys. Lett.* **103**, 173905 (2013).
- [19] E. Moulin, M. Steltenpool, M. Boccard, L. Garcia, G. Bugnon, M. Stuckelberger, E. Feuser, B. Niesen, R. van Erven, J.-W. Schüttauf, F.-J. Haug, and C. Ballif, *IEEE J. Photovolt.* **4**, 1177 (2014).